Uncertainty Quantification of LWR by Random Sampling Method with STREAM/RAST-K

Yongmin Jo[a], Sooyoung Choi[a], Jiwon Choe[a], Yunki Jo[a], Jiankai Yu[a], Deokjung Lee[a*]
[a]*Department of Nuclear Engineering, Ulsan National Institute of Science and Technology*
50 UNIST-gil, Ulsan, 44919, Republic of Korea
[*]*Corresponding author: deokjung@unist.ac.kr*

1. Introduction

For the safety of nuclear power plant (NPP) operation, the accuracy of core simulation is very important. Nowadays, there are many powerful computer codes that can simulate the core quickly and reasonably using measured data. However, these codes usually do not include the effects of uncertainties in the input data used in the calculations. So, for precise predictions, the data uncertainties should be considered.

In this paper, the important nuclear data in reactor core simulations are considered by assuming the variations in the input data follow the standard normal distribution. Because each nuclear data is not independent, the simulation should consider the relationship between them. For this purpose, there are random sampling method that use covariance of nuclear data to reflect the above relationship and make perturbed data sets. By using these data sets, core simulations of a commercial LWR are carried out many times and the uncertainties of core properties are quantified.

2. Method

In this section, the procedure of applying covariance data to vary the nuclear data is described [1, 2]. Also, the practical reactor model is briefly introduced.

2.1. Covariance data matrix

Covariance matrix shows the relationship between two nuclear data. In this paper, the multi-group covariance data generated by NJOY code are treated as one covariance matrix to consider the whole covariance data as a symmetric matrix in one step.

$$\mathbf{C} = \begin{bmatrix} \mathbf{C}_{a,a} & \mathbf{C}_{a,b} & \cdots & \cdots & \mathbf{C}_{a,z} \\ \mathbf{C}_{b,a} & \mathbf{C}_{b,b} & & & \vdots \\ \vdots & & \ddots & & \vdots \\ \vdots & & & \mathbf{C}_{y,y} & \mathbf{C}_{y,z} \\ \mathbf{C}_{z,a} & \cdots\vdots & \cdots & \mathbf{C}_{z,y} & \mathbf{C}_{z,z} \end{bmatrix}. \qquad (1)$$

In this covariance matrix, the element, $C_{a,a}$ represents multi-group covariance between nuclear data expressed by its subscripts. If there is no relation between two nuclear data, then the corresponding element of the covariance matrix is zero.

This paper considers 4-types of nuclear data; scattering, fission, capture cross sections and nu-bar. For the cross-section data, the covariance data are generated by NJOY 99 with ENDF/B-VII.1 and the nu-bar covariance data are generated by NJOY 2012 with the same library [3].

2.2. Random sampling for nuclear data

For the variable, z that obeys standard normal distribution, the normal distribution that have α, β^2 as its mean and variance can be generated by

$$x = \beta \times z + \alpha. \qquad (2)$$

Likewise, for the multivariate distribution vector **z** that include z following standard normal distribution as element, the multivariate distribution **x** can be generated by

$$\mathbf{x} = \mathbf{Az} + \boldsymbol{\mu}, \qquad (3)$$

where $\boldsymbol{\mu}$ is mean vector of **x** and **A** is square matrix that satisfy the Eq. (4) [1].

$$\mathbf{C} = \mathbf{AA}^{\mathbf{T}}. \qquad (4)$$

The **A** matrix can be solved by singular value decomposition of symmetric matrix **C** .

$$\mathbf{C} = \mathbf{U\Sigma U}^{\mathbf{T}}, \qquad (5)$$

where **U** is a set of orthonormal eigenvectors of $\mathbf{CC}^{\mathbf{T}}$**, which** means that $\mathbf{C}^2$ and $\boldsymbol{\Sigma}$ are diagonal matrix whose elements are also square roots of non-zero eigenvalues of $\mathbf{C}^2$. So, the **A** matrix can be expressed as in Eq. (6) [1, 2].

$$\mathbf{C} = \mathbf{U}\sqrt{\boldsymbol{\Sigma}}\sqrt{\boldsymbol{\Sigma}}\mathbf{U}^{\mathbf{T}} = (\mathbf{U}\sqrt{\boldsymbol{\Sigma}})(\mathbf{U}\sqrt{\boldsymbol{\Sigma}})^{\mathbf{T}}, \qquad (6)$$

$$\therefore \mathbf{A} = \mathbf{U}\sqrt{\boldsymbol{\Sigma}}. \qquad (7)$$

Therefore, the random sampled set, **x** is

$$\mathbf{x} = \mathbf{U}\sqrt{\boldsymbol{\Sigma}}\mathbf{z} + \boldsymbol{\mu}, \qquad (8)$$

2.3. Nuclear data library perturbation

In this study, nuclear data are perturbed with relative covariance matrix (absolute covariance matrix divided by expected value of nuclear data) given as [3]

$$\mathrm{rcov}(x,y) \equiv \frac{\mathrm{cov}(x,y)}{x_0 y_0}, \qquad (9)$$

where

$$x_0 \equiv \mathrm{E[x]}, \text{ and } y_0 \equiv \mathrm{E[y]}.$$

Here, x, y mean probability distribution and E is expectation operator.

So, from above equation (8), the elements of set **x** can be expressed simply.

$$x_{t,g} = (\mathbf{U}\sqrt{\mathbf{\Sigma}}\mathbf{z} + \boldsymbol{\mu})_{t,g} \times \sigma_{t,g}, \qquad (10)$$

where

x is perturbed elements of set $\mathbf{x}$,
σ is unperturbed elements of nuclear data set,
$\boldsymbol{\mu}$ is vector whose elements are 1,
t is type of nuclear data,
and
g is group of nuclear data.

2.4. Sampled nuclides

For the simulation of light water reactor, there are nuclides that largely affect the core calculation result. This kind of nuclides are already researched in other papers [4]. In this present paper, the 28 nuclides Table 1 are considered by using ENDF/B-VII.1.

Table1 The list of most important nuclide in LWR calculation [4].

H-1	B-10	B-11	O-16	Zr-91
ZR-96	Rh-103	Xe-135	Sm-149	Gd-155
Gd-157	U-234	U-235	U-236	U-237
U-238	Np-237	Np-239	Pu-238	Pu-240
Pu-241	Pu-242	Am-241	Am-242*	Am-243
Cm-242	Cm-244	Cm-245		

2.5 Core model

A commercial core design of APR-1400 and fuel model PLUS7 is used in this research. Specifically, the first cycle that has 241 feed fuel assemblies with different enrichment and number of gadolinia pin is analyzed.

	J	K	L	M	N	P	R	S	L
9	A	A	C	A	B	A	B	C	B
10	A	B	A	B	A	B	A	B	C
11	C	A	C	A	C	A	C	B	B
12	A	B	A	B	A	B	A	B	C
13	B	A	C	A	C	A	B	C	
14	A	B	A	B	A	B	C	C	
15	B	A	C	A	B	C	C		
16	C	B	B	B	C	C			
17	B	C	B	C					

Fig.1 The APR-1400 FA pattern

3. Numerical results

In this part, important core properties are calculated to obtain the mean and uncertainty. Totally, there are 500 samples and each of them is perturbed by random sampling method. From this perturbed nuclear data sets, 500 calculations are performed for the same model and the mean value and 1σ for some core properties are evaluated as uncertainty.

For the core simulation, STREAM, STORA, and RAST-K 2.0 are used and briefly described [5].

STREAM is a 2D lattice code that solves the neutron transport equation by the method of characteristics (MOC). STREAM calculates 2-group cross section data from perturbed nuclear data sets.

The STORA code have a role to connect STREAM and RAST-K 2.0 by gathering STN files that contains STREAM results which will be used by RAST-K.

RAST-K simulate whole core models by using 3D 2-group unified nodal method (UNM).

3.1. Critical boron concentration

The critical boron concentration (CBC) is calculated 500 times. Fig.2 shows the samples mean and its standard deviation (1σ).

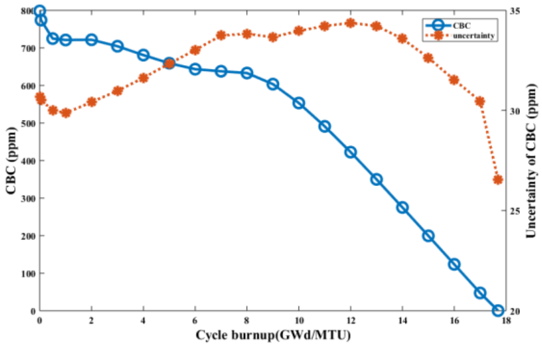

Fig.2 Critical boron concentration and its uncertainty (1σ).

The uncertainty CBC shows some trends by following the amount of U-235, boron and fission products change that play a big role in core uncertainty analysis.

At the beginning of cycle (BOC), the amount of U-235 and boron decrease. It makes the decrease of uncertainty because they strongly affect to core uncertainty. However, the uncertainty starts to increase until a certain burn-up point because of the effect of fission product generation that acts positively on the uncertainty and surpasses the impact of decreased U-235 and boron. However, there are one more turning point for uncertainty. It seems like mainly due the boron decrease that makes the uncertainty also decrease.

3.2. Axial power distribution

The axial power distribution and the uncertainty at BOC and EOC are shown in Fig.3.

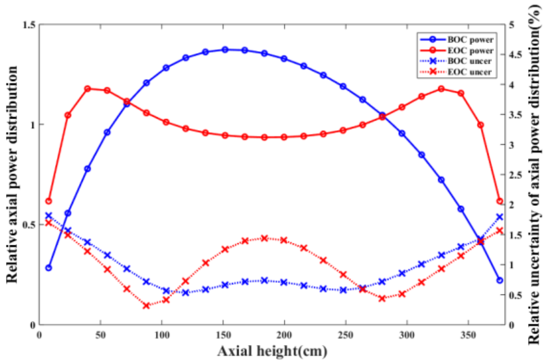

Fig.3 Relative axial power distribution and its relative uncertainty at EOC.

The interesting point from the two graphs is that there are increasing trends for the middle part of core. This trend is obvious because during the cycle burn-up, the fission happens mainly in the core middle part, and there are more trans-uranium nuclides generation causing more drastic curve in the uncertainty trend.

3.3. Radial distribution

For the radial power and burn-up distributions, the uncertainty is calculated as relative uncertainty (%). Each of these shows similar trend at BOC and EOC. Identical to the CBC case, at BOC, the uncertainty value for whole region show higher value than at EOC.

	J	K	L	M	N	P	R	S	L
9	0.94								
	1.54								
10	0.9	1							
	1.45	1.31							
11	1.08	0.9	1.11						
	1.16	1.22	0.99						
12	0.92	1.04	0.92	1.04					
	1.05	0.97	0.93	0.72					
13	1.15	0.96	1.13	0.93	1.14				
	0.66	0.73	0.57	0.52	0.17				
14	0.98	1.17	0.96	1.06	0.94	1.02			
	0.44	0.32	0.33	0.14	0.09	0.5			
15	1.06	0.96	1.13	0.95	1.12	1.05	0.81		
	0.13	0.05	0.2	0.28	0.66	0.9	0.81		
16	1.11	1.03	1.06	0.99	1.07	0.78		FA POWER	
	0.66	0.64	0.7	0.74	0.9	0.87		Rel.Uncer(%)	
17	0.99	1.05	0.92	0.74					
	0.93	0.96	0.93	0.77					

Fig.4 Normalized FA power and its relative uncertainty (%) at BOC. In this, BOC mean initial burn-up, 0.0500 GWd/MTU.

	J	K	L	M	N	P	R	S	L
9	0.05								
	1.5								
10	0.05	0.05							
	1.41	1.27							
11	0.05	0.05	0.06						
	1.13	1.19	0.96						
12	0.05	0.05	0.05	0.05					
	1.03	0.95	0.91	0.71					
13	0.06	0.05	0.06	0.05	0.06				
	0.65	0.72	0.56	0.52	0.17				
14	0.05	0.06	0.05	0.05	0.05	0.05			
	0.438	0.31	0.33	0.15	0.09	0.48			
15	0.05	0.05	0.06	0.05	0.06	0.05	0.04		
	0.13	0.05	0.19	0.27	0.65	0.88	0.79		
16	0.06	0.05	0.05	0.05	0.05	0.04		FA BU	
	0.65	0.62	0.69	0.73	0.89	0.86		Rel.Uncer(%)	
17	0.05	0.05	0.05	0.04					
	0.92	0.95	0.92	0.76					

Fig.5 Burn-up distribution and its relative uncertainty (%) at BOC. In this, BOC mean initial burn-up, 0.0500 GWd/MTU.

At the BOC, the uncertainty of power and burn-up shows very similar value and trend. The reason is that the random sampling for the 28 nuclides is enough to describe the core at the BOC. However, for the EOC case, it shows very different result because there are many nuclides in the core at the EOC state which are not considered in random sampling.

	J	K	L	M	N	P	R	S	L
9	0.89								
	0.28								
10	0.92	1.1							
	0.29	0.32							
11	1.16	0.95	1.18						
	0.32	0.25	0.27						
12	0.94	1.12	0.96	1.13					
	0.2	0.21	0.18	0.14					
13	1.1	0.94	1.17	0.97	1.2				
	0.16	0.19	0.14	0.19	0.11				
14	0.94	1.12	0.96	1.14	0.97	1.14			
	0.24	0.16	0.21	0.12	0.19	0.14			
15	1.15	0.97	1.19	0.95	1.1	1.07	0.77		
	0.16	0.21	0.12	0.18	0.12	0.25	0.39		
16	1.18	1.11	1.09	0.99	0.91	0.69		FA POWER	
	0.16	0.13	0.12	0.16	0.26	0.43		Rel.Uncer(%)	
17	0.83	0.86	0.78	0.66					
	0.21	0.22	0.26	0.45					

Fig.6 Normalized FA power and its relative uncertainty (%) at EOC.

	J	K	L	M	N	P	R	S	L
9	16.15								
	1.26								
10	16.40	19.43							
	1.27	1.26							
11	20.65	16.97	21.25						
	1.24	1.25	1.22						
12	17.05	20.01	17.18	20.10					
	1.24	1.23	1.24	1.23					
13	20.51	17.22	21.05	17.13	21.13				
	1.17	1.21	1.21	1.22	1.21				
14	17.26	20.62	17.18	19.81	16.78	18.94			
	1.189	1.16	1.2	1.22	1.21	1.29			
15	20.14	17.24	20.71	16.48	18.97	17.81	12.86		
	1.22	1.2	1.22	1.2	1.24	1.34	1.29		
16	20.35	19.11	18.71	16.74	16.03	11.71			
	1.28	1.28	1.27	1.27	1.22	1.26			
17	15.01	15.67	13.80	11.32					
	1.2	1.2	1.22	1.24					

FA BU
Rel.Uncer(%)

Fig.7 Burn-up distribution and its relative uncertainty (%) at EOC.

3.4. Rod worth

APR-1400 has seven control rod groups that include two shutdown groups (A, B). In this, the rod worth is analyzed as group worth for the BOC and EOC state with HFP, Eq. Xe condition.

Table2 Group worth and its relative uncertainty (%).

Group	BOC HFP, Eq. Xe	
	Group worth±1σ (pcm)	Relative Uncertainty (%)
5	300±3.72	1.24
4	405±2.80	0.69
3	760±9.77	1.28
2	977±7.66	0.78
1	1436±26.51	1.84
A	4640±27.68	0.59
B	5195±22.29	0.42

Table3 Group worth and its relative uncertainty (%).

Group	EOC HFP, Eq. Xe	
	Group worth±1σ (pcm)	Relative Uncertainty (%)
5	352±2.55	0.72
4	459±2.82	0.61
3	774±4.86	0.62
2	1019±5.69	0.55
1	1425±13.36	0.93
A	4174±35.60	0.85
B	4549±59.62	1.3

The whole rod worth results show the uncertainty less than 2%. However, there is a new trend that the uncertainty of BOC case is higher than EOC case which are reversed result trend. The reason is that at BOC, there are smaller number of neutrons than that of EOC, and if the neutron is absorbed by poison material, it causes bigger fluctuations, meaning bigger uncertainty at BOC state.

5. Conclusion

This paper presents the calculated uncertainties of a commercial LWR by using random sampling method and STREAM/RASTK codes. Uncertainties of various core safety parameters are quantified and the uncertainty quantification capability of STREAM/RASTK codes was successfully demonstrated. For the further study, more isotopes and reaction types will be considered such as fission spectrum, χ.

6. Acknowledgement

This research was supported by the project(L17S018000) by Korea Hydro & Nuclear Power Co. Ltd.

REFERENCES

[1] Akio Yamamoto, Kuniharu Kinoshita, Tomoaki Watanabe, Tomohiro Endo, Yasuhiro Kodama, Yasunori Ohoka, Tadashi Ushio & Hiroaki Nagano, Uncertainty Quantification of LWR Core Characteristics Using Random Sampling Method, Nuclear Science and Engineering, 181:2, 160-174, 2012.
[2] Tomoaki Watanabe, Tomohiro Endo, Akio Yamamoto, Yasuhiro Kodama, Yasunori Ohoka & Tadashi Ushio Cross section adjustment method based on random sampling technique, Journal of Nuclear Science and Technology, 51:5, 590-599, 2014.
[3] Muir WD, Boicourt MR, Kahler CA, The NJOY nuclear data processing system, version 2012. Los Alamos, USA: Los Alamos National Laboratory; 2012.
[4] Ivanov, K., Avramova, M., Kamerow, S., Kodeli, I., Sartori, E., Ivanov, E., & Cabellos, O., Benchmarks for Uncertainty Analysis in Modelling (UAM) for the Design, Operation and Safety Analysis of LWRs, Volume I: Specification and Support Data for Neutronics Cases, pp.20-21, Nuclear Energy Agency of the OECD (NEA), 2013.
[5] Jiwon Choe, Sooyoung Choi, Minyong Park, Peng Zhang, Ho Cheol Shin, Hwan Soo Lee, Deokjung Lee, Validation of the UNIST STREAM/RAST-K Code System with OPR -1000 Multi-cycle Operation, RPHA17, 2017.